JCB Article

Fibroblast growth factor–specific modulation of cellular response by syndecan-4

Arie Horowitz, Eugene Tkachenko, and Michael Simons

Angiogenesis Research Center and Section of Cardiology, Department of Medicine, Dartmouth Medical School, Lebanon, NH 03756

Proteoglycans participate in growth factor interaction with the cell surface through their heparan sulfate chains (HS), but it is not known if they are otherwise involved in growth factor signaling. It appears now that the syndecan-4 core protein, a transmembrane proteoglycan shown previously to bind phosphatidylinositol 4,5-bisphosphate (PIP_2) and activate PKCα, participates in mediating the effects of fibroblast growth factor (FGF)2 on cell function. Mutations in the cytoplasmic tail of syndecan-4 that either reduced its affinity to PIP_2 (PIP_2^-) or disrupted its postsynaptic density 95, disk large, zona occludens-1 (PDZ)-dependent binding (PDZ^-) produced a FGF2-specific dominant negative phenotype in endothelial cells as evidenced by the marked decline of their migration and proliferation rates and the impairment of their capacity to form tubes. In both cases, the molecular mechanism was determined to consist of a decrease in the syndecan-4–dependent activation of PKCα. This decrease was caused either by inhibition of FGF2-induced syndecan-4 dephosphorylation in the case of the PDZ^- mutation or by disruption of basolateral targeting of syndecan-4 and its associated PDZ-dependent complex in the case of the PIP_2^- mutation. These results suggest that PKCα activation and PDZ-mediated formation of a serine/threonine phosphatase-containing complex by syndecan-4 are downstream events of FGF2 signaling.

Introduction

The participation of heparan sulfate (HS)* chains in binding numerous soluble ligands and extracellular matrix proteins (Bernfield et al., 1999) drew increased attention once HS presence on the cell surface was shown to be required for fibroblast growth factor (FGF)2-dependent cell growth (Rapraeger et al., 1991). The list of HS-binding soluble ligands has grown significantly, culminating recently in the finding that syndecan-1–attached HS chains promote the tumorigenic response to Wnt-1 (Alexander et al., 2000).

The potential role of the HS-carrying core of the proteoglycans in mediating the cellular response to growth factors received little attention, however, despite earlier indications of their response to extracellular signals, such as the recruitment of syndecan-4 to focal adhesions (Woods and Couchman, 1994; Baciu and Goetinck, 1995). The possibility of fulfilling specific functional roles seems particularly relevant to the syndecan core proteins, all of which share a distinct and highly conserved cytoplasmic tail. One of the motifs common to all the syndecans is a COOH-terminal postsynaptic density 95, disk large, zona occludens-1 (PDZ)-binding motif now known to bind at least four PDZ domain–containing partners (Grootjans et al., 1997; Cohen et al., 1998; Hsueh et al., 1998; Ethell et al., 2000; Gao et al., 2000). Similar to other PDZ proteins, these binding partners very likely serve as adaptors between the syndecans and additional members of larger complexes.

Syndecan-4, the most widely spread member of the family, differs in its sequence from the other three syndecans by a unique phosphatidylinositol 4,5-bisphosphate (PIP_2)–binding seven-residue motif located in the middle of its 28–amino acid–long cytoplasmic tail (Lee et al., 1998; Horowitz et al., 1999). Syndecan-4 has been implicated in signal transduction (Volk et al., 1999) and the activation of PKCα (Oh et al., 1997b). PIP_2 appears to underlie the signaling activity of the cytoplasmic tail of syndecan-4, serving as a binding interface (Horowitz et al., 1999), an essential cofactor for PKCα activation (Oh et al., 1998), and a facilitator of the tail's multimerization (Oh et al., 1997a). These properties are regulated by the phosphorylation of S^{183} located four residues away from the NH_2 terminus of the PIP_2-binding motif (Horowitz and Simons, 1998a). Once phosphory-

Address correspondence to Arie Horowitz, Angiogenesis Research Center and Section of Cardiology, HB-7504, Dept. of Medicine, Dartmouth Medical School, One Medical Center Dr., Lebanon, NH 03756. Tel.: (603) 650-2635. Fax: (603) 653-0510. E-mail: arie.horowitz@dartmouth.edu

*Abbreviations used in this paper: EGF, epithelial growth factor; EGFP, enhanced green fluorescent protein; FACS, fluorescence-assisted cell sorting; FGF, fibroblast growth factor; HA, hemagglutinin; HS, heparan sulfate; PDZ, postsynaptic density 95, disk large, zona occludens-1; PIP_2, phosphatidylinositol 4,5-bisphosphate; PP1/2A, protein phosphatase type 1/2A; RFPEC, rat fat pad endothelial cell; R-PE, red pycoerythrin.

Key words: FGF; PDZ; signal transduction; syndecan-4; PKC

lated, the affinity of the cytoplasmic tail for PIP_2 and its capacities to oligomerize and activate PKCα in the presence of PIP_2 are sharply reduced (Simons and Horowitz, 2001).

Given the HS dependence of the activity of several growth factors and the in vivo–observed increase in syndecan-4 expression during growth factor-regulated healing from injury (Gallo et al., 1994; Nikkari et al., 1994; Li et al., 1997), we asked whether the molecular attributes of syndecan-4 listed above are relevant to growth factor signaling. Using FGF2 as an HS-binding growth factor prototype, we found that disruption of either the PIP_2 or PDZ-binding domains of syndecan-4 conferred a dominant negative phenotype in regard to this growth factor but not to serum or epithelial growth factor (EGF)- and PDGF-induced response.

Therefore, these data suggest that syndecan-4 selectively regulates FGF2 signaling in endothelial cells.

Results

Site-directed mutations in syndecan-4 confer dominant negative effects on FGF2 signaling in endothelial cells

We addressed the potential role of syndecan-4 in regulating the cellular response to FGF2 by transfecting rat fat pad endothelial cells (RFPECs), which express syndecan-4 endogenously (Kojima et al., 1992), with hemagglutinin (HA)-tagged wild-type (WT) (S4) syndecan-4 or with HA-tagged syndecan-4 constructs mutated at two key sites (Fig. 1 A). In the first construct (PIP_2^-), the three consecutive residues $Y^{192}KK$ in the cytoplasmic tail of syndecan-4 were mutated to LQQ, a mutation that drastically reduces the PIP_2 affinity of the cytoplasmic tail and inhibits its PIP_2-mediated activation of PKCα (Horowitz et al., 1999). In another construct (PDZ^-), the COOH-terminal residue (A^{202}) was deleted, thereby abolishing PDZ-dependent binding of syndecan-4 (Songyang et al., 1997). Finally, a PIP_2^-/PDZ^- construct combined the features of the other two constructs.

To measure the expression level of the introduced constructs and the effect of exogenous construct expression on endogenous syndecan-4 levels, we immunoblotted total cell lysates from each of the cell lines with antibodies to syndecan-4 and HA (Fig. 1 B). The syndecan-4 immunoblot represents the sum of endogenous and transfected syndecan-4 proteins, whereas the HA immunoblot assesses the amount of transfected syndecan-4. The immunoblots showed on average a twofold increase in the expression level of the exogenous constructs over the endogenous syndecan-4 protein in the transfected cell lines, excluding the PIP_2^- cells where the mutated syndecan-4 variant is not recognized by the antibody against the cytoplasmic tail used in these experiments, since the LQQ mutation disrupts its epitope (unpublished data).

To find whether these mutations perturbed FGF2 signaling, we examined several potentially susceptible cell functions. Migration rate in response to FGF2 treatment was measured by a wounding assay of confluent cell monolayers. The migration rates of cells expressing either PIP_2^- or PDZ^- syndecan-4 mutants were similar to each other and threefold lower than the migration rate of vector-transfected RFPECs (Fig. 2 A). At the same time, migration of cells carrying the combined PIP_2^-/PDZ^- mutation was not different from controls. In agreement with our previous observations (Volk et al., 1999), the migration rate of RFPECs overexpressing S4 was even higher than vector-transfected cells (relative gap closure of 0.34 ± 0.09 versus 0.27 ± 0.03, respectively; $n = 12$, $p = 0.023$). Cell growth in response to FGF2 over a period of 3 d was measured by proliferation assays with the same cell clones used in the migration assays. Cells expressing either the PIP_2^- or PDZ^- mutants had 3–5-fold lower proliferation rates in comparison to vector-transfected cells, whereas cells expressing the

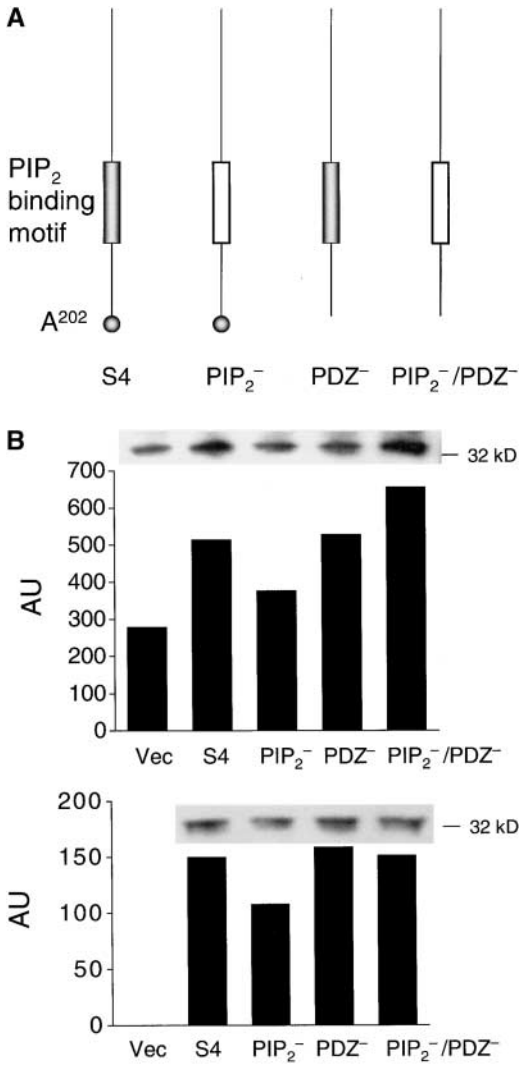

Figure 1. **Syndecan-4 mutants and their expression level in RFPECs.** (A) Schemes of syndecan-4 cytoplasmic tail constructs used in the study. From left to right: WT cytoplasmic tail (S4, solid cylinder; PIP_2-binding domain, solid sphere; COOH-terminal A^{202} residue), PIP_2^- ($Y^{192}KK$ to LQQ) mutation (void cylinder), PDZ^- (deletion of the COOH-terminal A^{202} residue) mutation, and PIP_2^-/PDZ^- (combination of both mutations). (B) Protein levels of exogenous and endogenous syndecan-4 in transfected cell clones. (Top) Immunoblots for total syndecan-4 protein levels using antiserum specific to the cytoplasmic tail of syndecan-4, and a histogram representing the densitometric values of each band (in arbitrary units). (Bottom) As above, using HA tag antibody. Aliquots of cell lysate containing equal masses of total protein were immunoprecipitated from each cell group with antiserum specific to the ectoplasmic tail of syndecan-4. Glycosaminoglycan chains were digested before gel electrophoresis.

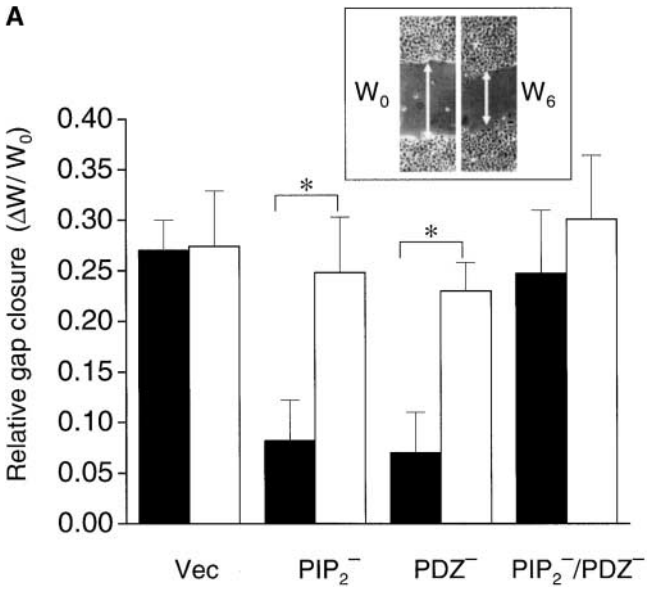

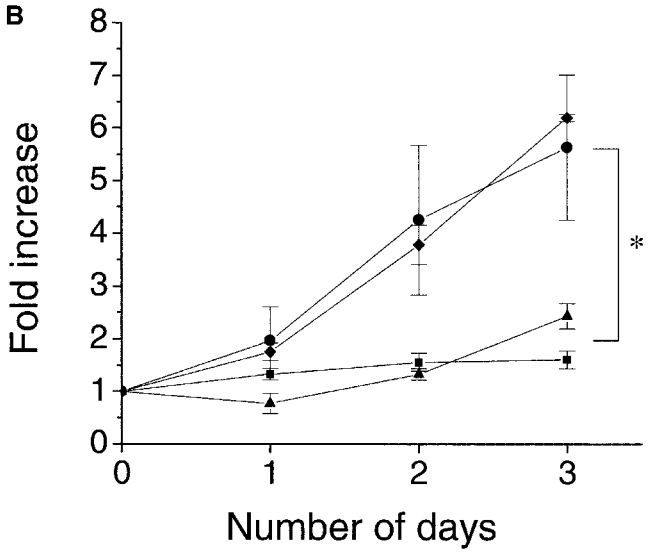

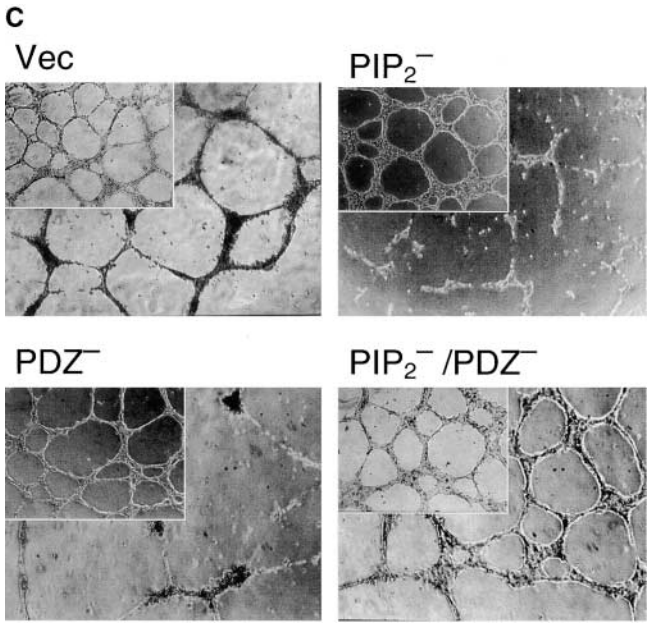

PIP_2^-/PDZ^- mutation had the same proliferation rate as vector controls, a pattern similar to the results of the migration assays (Fig. 2 B). Finally, tube formation on extracellular matrix basement in response to FGF2 by cell clones expressing the PIP_2^- or PDZ^- syndecan-4 mutations, but not the PIP_2^-/PDZ^- mutation, was also markedly impaired in comparison with the continuous and articulated tube networks formed by vector-transfected cells (Fig. 2 C) or by S4-overexpressing RFPECs (unpublished data).

The combined results of the migration, proliferation, and tube formation experiments indicate that both the LQQ substitution and the A^{202} deletion conferred a dominant negative phenotype on RFPECs when coexpressed with endogenous syndecan-4. This effect was FGF2 specific, since when performed in the presence of 10% serum (Fig. 2, A and C) or in the presence of either EGF or PDGF AB (25 ng/ml each [unpublished data]) migration and tube formation by PIP_2^- and PDZ^- cells did not differ from those of vector-transfected cells.

PIP_2^- mutation impairs syndecan-4 targeting to the basolateral region

To elucidate the mechanism of the dominant negative effect of the mutations in the cytoplasmic tail of syndecan-4, we compared the cellular distribution of each mutated syndecan-4 variant to that of the endogenous molecule. Staining of untransfected RFPECs with the antibody to syndecan-4 demonstrated the presence of the proteoglycan along the cell borders and in the perinuclear region (Fig. 3, top). S4 expressed in RFPECs assumed a similar distribution (Fig. 3, bottom). The perinuclear location coincided with the Golgi apparatus as shown by overlap with the staining for the Golgi scaffold protein GM130 (Nakamura et al., 1995).

Both the PIP_2^- and PIP_2^-/PDZ^- syndecan-4 variants maintained their Golgi localization but were no longer present in the basolateral region (Fig. 4, A and C, respectively). In contrast with the cellular distribution of the PIP_2^- and PIP_2^-/PDZ^- syndecan-4 mutants, the distribution of the PDZ^- mutant (Fig. 4 B) did not differ from that of the endogenous syndecan-4, indicating that syndecan-4 is targeted to the basolateral region by its association with PIP_2 rather than with a PDZ protein.

Figure 2. **Effects of syndecan-4 mutations on cell function.** (A) Migration of RFPECs as measured in "wounding" assays (inset). Cells were starved in 0.5% FBS for 24 h, scratched, and incubated for another 6 h either with 0.5% FBS and 20 ng/ml FGF2 (black bars) or with 10% FBS alone (white bars). Gap size was measured immediately before (W_0) and after (W_6) the 6-h incubation period ($\Delta W = W_0 - W_6$). Data shown as mean ± SD ($n = 12 \div 18$; $^*p < 0.05$). (B) Fold increase in cell number relative to day 0 as measured in RFPEC proliferation assays. Cells were starved as above and then treated with 20 ng/ml FGF2 ($n = 3$). Cells were counted immediately before FGF2 application and at 24, 48, and 72 h after it. Data shown as mean ± SD (n = 4; $^*p < 0.05$ [◆, vector-transfected control cells; ▲, PIP_2^- cells; ■, PDZ^- cells; ●, PIP_2^-/PDZ^- cells]). (C) Tube formation assays on extracellular matrix basement (Matrigel™; Beckton Dickinson). Cells were starved as above, then treated for 24 h either with 0.5% FBS and 20 ng/ml FGF2 or with 10% FBS alone (insets), and imaged immediately. Each cell line was assayed in duplicate. Note that all cell lines formed normal tube networks when treated with 10% FBS.

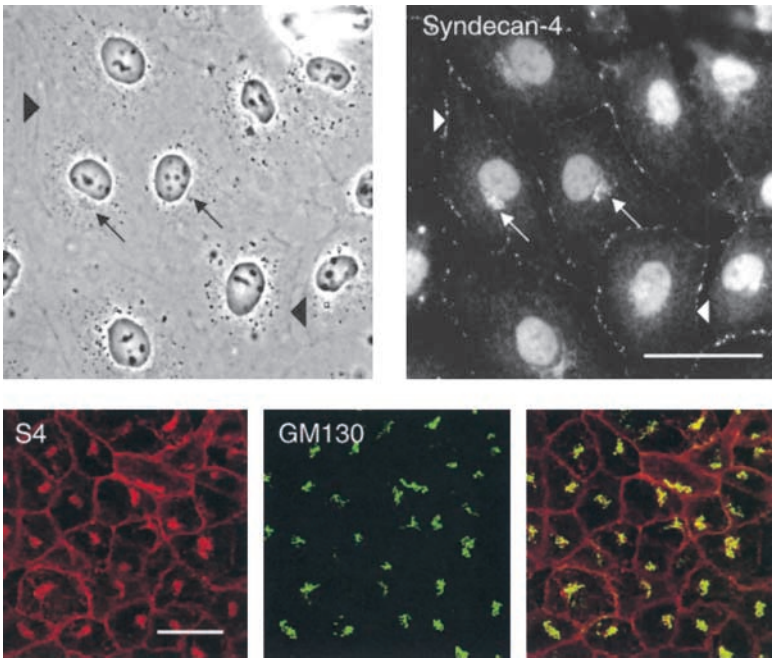

Figure 3. **Cellular distribution of endogenous and transfected syndecan-4 in RFPECs.** (Top) Phase (left) and immunofluorescence (right) images of the same untransfected RFPECs labeled with 1:50 diluted syndecan-4 cytoplasmic tail antiserum. Arrows point to the Golgi apparatus, and arrowheads point to cell junctions. Nuclear staining on the right is due to nonspecific immunolabeling. (Bottom) Confocal immunofluorescence images of RFPECs doubly labeled with 1 μg/ml HA antibody (Roche) and 2.5 μg/ml antibody to GM130 (Transduction Laboratories), showing the distribution of HA-tagged WT syndecan-4 (S4, left), GM-130 Golgi marker (middle), and an overlay of both images. Bars, 25 μm. Note the distribution of both endogenous and WT overexpressed syndecan-4 (S4) along cell junctions and in the Golgi apparatus.

To further examine the effect of the PIP_2^- mutation on the surface targeting of syndecan-4, the S4, PIP_2^-, and PIP_2^-/PDZ^- variants were transfected into RFPECs via a bicistronic enhanced green fluorescent protein (EGFP)-expressing plasmid. Each cell group was scanned at both 488 nm, the EGFP emission wavelength, and 580 nm, the emission wavelength of the red pycoerythrin (R-PE) fluorophore conjugated to the secondary antibody used to detect the HA-tagged exogenous syndecan-4. As shown in Fig. 5 A, cells transfected by S4 (Fig. 5 A, b) had high counts at both wavelengths, whereas cells expressing the PIP_2^- and PIP_2^-/PDZ^- mutants (Fig. 5 A, c and d, respectively) had low counts at 580 nm similar to the vector-transfected control cells (Fig. 5 A, a). Note that though the fraction of EGFP-expressing cells out of the total PIP_2^- cell population is low relative to the EGFP-expressing fractions in the other three the cell populations, the ratio between the cell fraction expressing both EGFP and PIP_2^- and the fraction expressing only EGFP (1:20) is similar to the corresponding ratio (1:25) in the PIP_2^-/PDZ^- cell population, whereas the ratio in the S4 cell population is much higher (1:3). These results confirm the conclusion drawn from the immunofluorescence experiments that the PIP_2^- syndecan-4 mutant is not present on the cell surface.

The sequestration of the PIP_2^--mutated syndecan-4 to the Golgi apparatus may potentially reduce the presence of endogenous syndecan-4 on the cell surface if the two could form heterooligomers. In that case, the lower responses of the PIP_2^- cells to FGF2 observed in the functional assays (Fig. 2) may result not only from the presence of the mutated form of syndecan-4, but more trivially, from the resulting deficit in the available FGF-binding sites along the syndecan-4–associated HS chains. To test this possibility, we quantified the amount of syndecan-4 present on the cell surface in vector-transfected and PIP_2^- cells by fluorescence-assisted cell sorting (FACS) using an antibody against the ectoplasmic domain of syndecan-4. Since we have shown already (Fig. 4 A and Fig. 5 A) that the PIP_2^- variant of

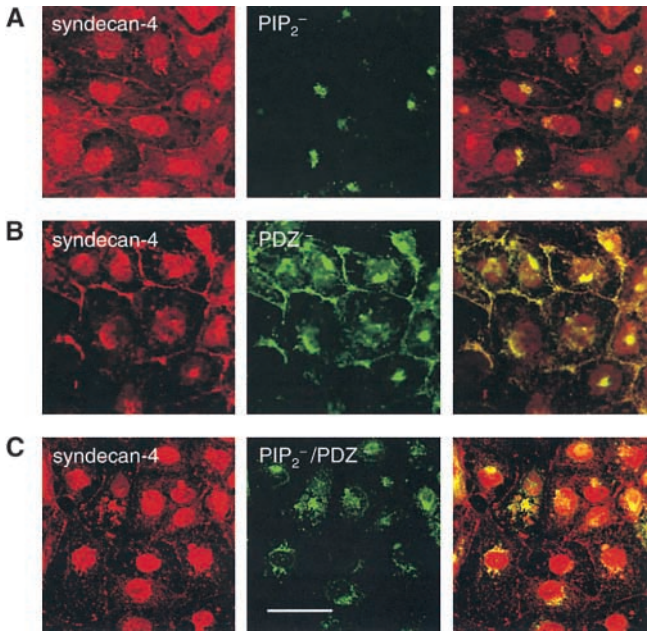

Figure 4. **The distribution of syndecan-4 mutants in RFPECs.** (A) PIP_2^--expressing cells doubly immunolabeled with syndecan-4 cytoplasmic tail antiserum (left) and HA antibody (middle). Note that the distribution of the PIP_2^- syndecan-4 (middle) was restricted to the Golgi, whereas native syndecan-4 (left) is localized both to the Golgi and along cell borders as in the top right of Fig. 3. Nuclei appear in this and in B and C due to nonspecific binding of the syndecan-4 antiserum. (B) PDZ^- cells doubly immunolabeled with syndecan-4 cytoplasmic tail antiserum (left) and HA antibody (middle). Note that the distribution of the PDZ^- syndecan-4 was similar to that of HA-tagged WT syndecan-4 in Fig. 3, bottom left. (C) PIP_2^-/PDZ^- cells doubly immunolabeled with syndecan-4 cytoplasmic tail antiserum (left) and HA antibody (middle). Note that the distribution of the PIP_2^-/PDZ^- syndecan-4 was similar to that of PIP_2^- syndecan-4 in Fig. 4 A, middle. Panels on the right are overlays of the left and middle. Bar, 25 μm.

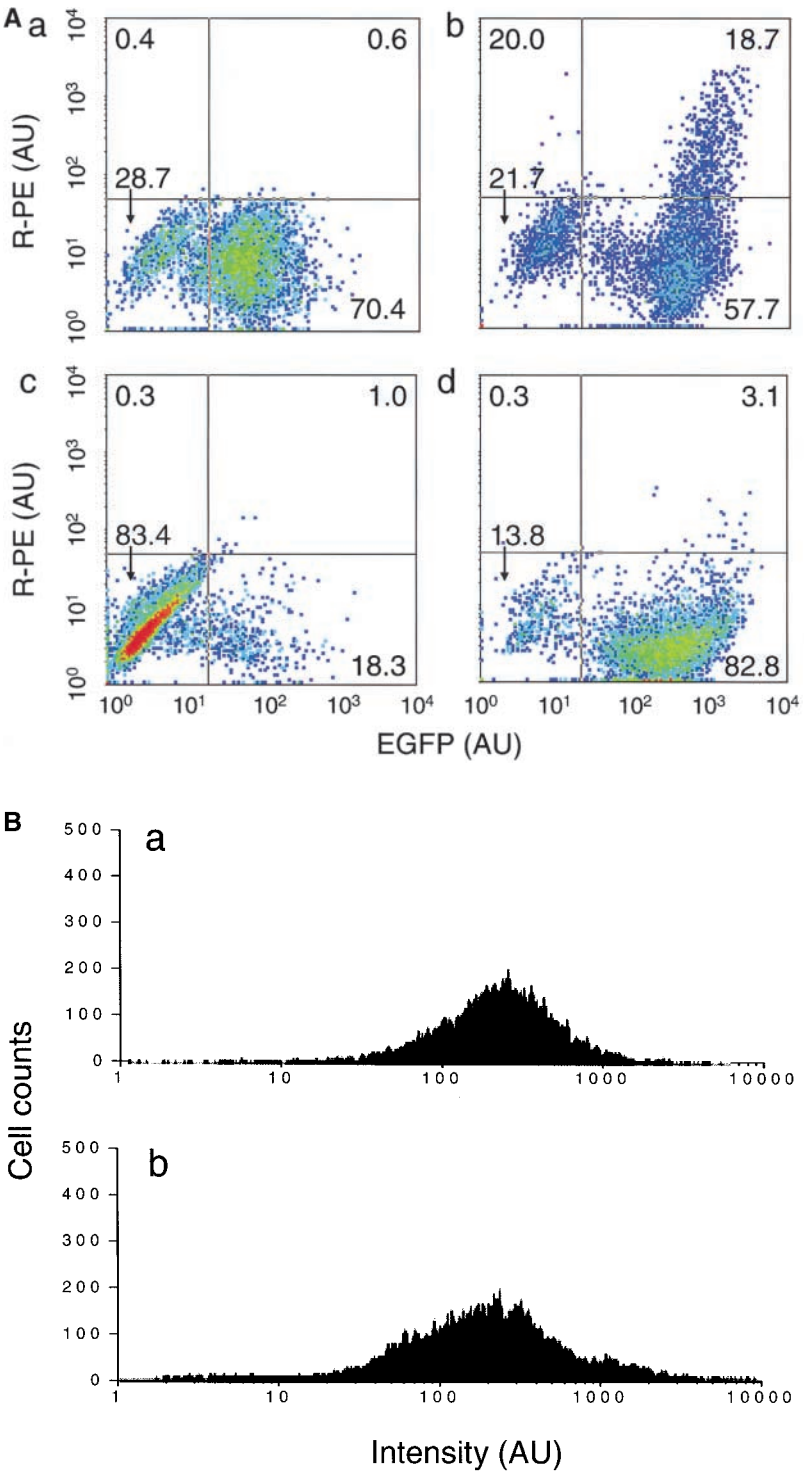

Figure 5. **FACS® analysis of exogenous and endogenous syndecan-4 expression levels.** (A) Distributions of pIRES2-EGFP vector-transfected (a), HA-WT–overexpressing (b), PIP_2^--transfected (c), and PIP_2^-/PDZ^--transfected cells (d) as a function of their fluorescence intensities at 488 nm (EGFP, horizontal axis, arbitrary units [AU]) and at 580 nm (R-PE, vertical axis), corresponding to the EGFP levels expressed either alone (a) or in tandem with each syndecan-4 variant (b, c, and d) and to the cell surface expression levels of the syndecan-4 variants, respectively. The quadrants were drawn so as to enclose near to 100% of control nontransfected cells (unpublished data) in the lower right quadrant. Numbers in the corners denote the percentage of the cell population in each quadrant. Quasi colors denote count density (red, high; blue, low). (B) Intensity distribution (in arbitrary units) of cells labeled with antiserum to the syndecan-4 ectoplasmic domain followed by anti–rabbit IgG-Alexa 594, showing the levels of cell surface expression of endogenous syndecan-4 in vector-transfected (a) and PIP_2^--expressing (b) cell lines.

syndecan-4 is not present on the cell surface, the antibody would detect only the endogenous syndecan-4. The FACS results (Fig. 5 B) show no significant differences between the amounts of syndecan-4 molecules present on the surface of vector-transfected and PIP_2^- cells.

PIP_2^- and PDZ^- mutations reduce syndecan-4–associated activity of PKCα

An established signaling role of syndecan-4 is the modulation of FGF2-stimulated PIP_2-dependent PKCα activity (Oh et al., 1997b; Horowitz and Simons, 1998a). Since the activity of this PKC isoenzyme has been linked previously to the promotion of cell growth (Kolch et al., 1993, 1996; Cai et al., 1997; Schonwasser et al., 1998; Lallena et al., 1999; Besson and Yong, 2000), migration (Harrington et al., 1997), and tube formation (Wang et al., 2002), we studied the effect of PIP_2^- and PDZ^- mutations on PKCα activity in these cells. To this end, we assayed the activity of PKCα coimmunoprecipitated with HA-tagged syndecan-4 core proteins from the RFPEC clones expressing S4, PIP_2^-, PDZ^-, or PIP_2^-/PDZ^- syndecan-4 constructs, before and after FGF2 stimulation.

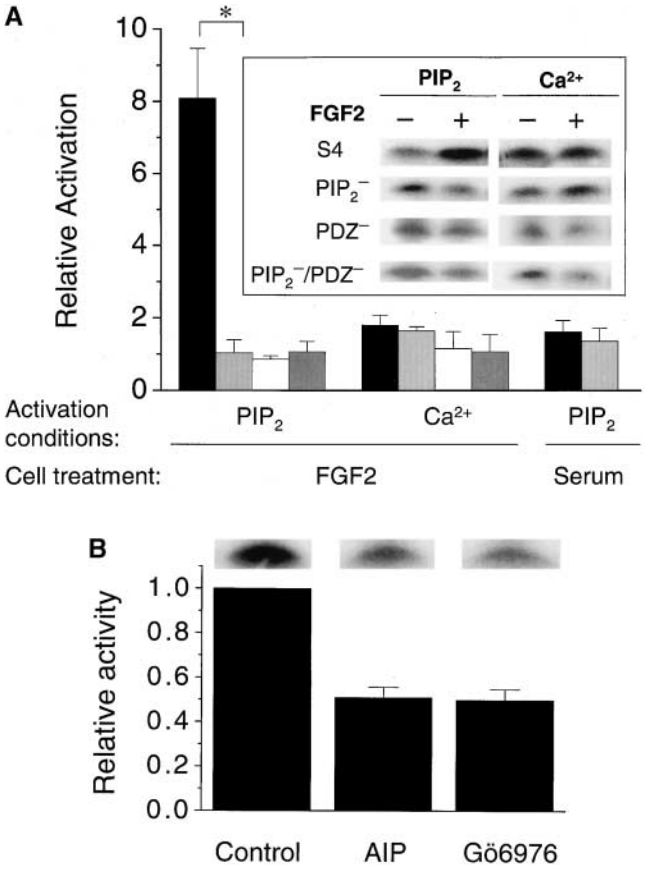

Figure 6. **Syndecan-4–associated kinase activities.** (A) Relative kinase activities of HA immunoprecipitates from RFPECs starved in 0.5% FBS for 24 h and then incubated for another 20 min either without or with 20 ng/ml FGF2, or with 10% FBS. Data shown is mean ± SD ($n = 3$) of the ratios between the kinase activity immunoprecipitated from FGF2- or FBS-treated cells and from nontreated cells of the same type. Note that the kinase activity of S4 cells was increased significantly by FGF2 treatment relative to other cell lines and that this relative increase was observed only when the immunoprecipitates where assayed in the presence of PIP_2^- but not when assayed in the presence of Ca^{2+}, phosphatidylserine, and diolein. Note also that the PIP_2-dependent kinase activities immunoprecipitated from S4 and PIP_2^--expressing cells did not significantly differ from each other when cells were treated with FBS instead of FGF2 (black bars, S4 cells; light gray bars, PIP_2^- cells; white bars, PDZ^- cells; dark gray bars, PIP_2^-/PDZ^- cells). (B) Effects of PKC autoinhibitor peptide (AIP, 100 nM) or of Gö6976 (10 nM) on kinase activities (mean ± SD, $n = 3$) of anti-HA immunoprecipitates from RFPECs in the presence of Ca^{2+}, phosphatidylserine, and diolein. Results are relative to the kinase activity of untreated control samples (insets in A and B are representative phosphoimages of PKCβI optimal substrate peptide bands used for quantifying the kinase activities of anti-HA precipitates).

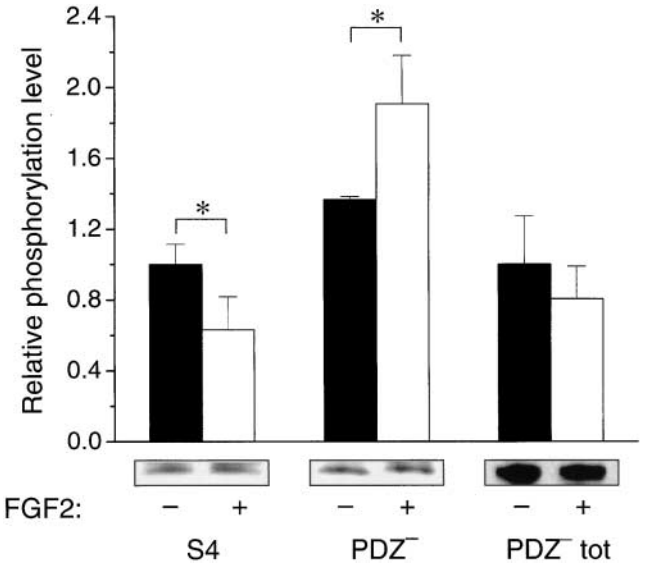

Figure 7. **Phosphorylation levels of syndecan-4.** Data shown is means ± SD ($n = 3$) of syndecan-4 phosphorylation levels measured as described in Materials and methods. Cells were incubated in 0.5% FBS either without (black bars) or with (white bars) 20 ng/ml FGF2 starting 2 h before radio labeling for a total of 4 h. Note the significant difference ($*p < 0.05$) between the phosphorylation levels of S4 and PDZ^- before and after FGF2 treatment (tot, total syndecan-4 population in the cell). (Insets) Immunoblots of representative samples from each cell group and condition.

FGF2 treatment increased syndecan-4/PIP_2-dependent PKCα activity eightfold in syndecan-4–overexpressing RFPECs relative to untreated cells of the same type (Fig. 6 A). On the other hand, syndecan-4–dependent PKCα activity in cells expressing PIP_2^-, PDZ^-, or PIP_2^-/PDZ^- syndecan-4 constructs was not increased by FGF2. No significant FGF2-induced relative increases in syndecan-4–associated kinase activities were observed when instead of PIP_2 the assays were done in the presence of Ca^{2+}, diacylglycerol, and phosphatidylserine. The absolute level of the Ca^{2+}-dependent activity of PKCα is typically higher by 20% than its activity in the presence of PIP_2 and the cytoplasmic tail of syndecan-4 (Horowitz and Simons, 1998a). The fact that the Ca^{2+}-dependent PKCα activities of all of the cell lines tested did not significantly differ from each other (Fig. 6 A), either with or without FGF2 treatment, indicates that similar amounts of PKCα were immunoprecipitated in all cases. Similar to the functional assays described above, the increase in the syndecan-4–associated kinase activity was specific to FGF2, since no significant differences were found between the syndecan-4–associated kinase activities in serum-treated versus untreated cells. Since the kinase activities were measured ratiometrically for each cell line (FGF2 or serum-treated versus untreated cells), they were not affected by variations between different cell lines in the absolute amounts of syndecan-4–associated PKCα.

Though the binding of PKCα to the cytoplasmic tail of syndecan-4 is well documented (Oh et al., 1997b; Horowitz and Simons, 1998a), we verified that the measured kinase activity in these assays was produced by a calcium-dependent PKC and not by other unidentified syndecan-4–associated kinases. Both the highly specific PKC autoinhibitor peptide (House and Kemp, 1987) and the cPKC inhibitor Gö6976 (Martiny-Baron et al., 1993) effectively suppressed the syndecan-4–associated kinase activity (Fig. 6 B).

PDZ^- syndecan-4 is hyperphosphorylated after FGF2 stimulation

Surprisingly, the FGF2-stimulated PKCα activity in cells transfected with the PDZ^- mutant was similar to that seen in cells transfected with the PIP_2^- mutant and much lower than in cells transfected with the native syndecan-4 construct (Fig. 6 A).

Given that the capacity of syndecan-4 to activate PKCα is sharply reduced by the phosphorylation of S^{183} in its cytoplas-

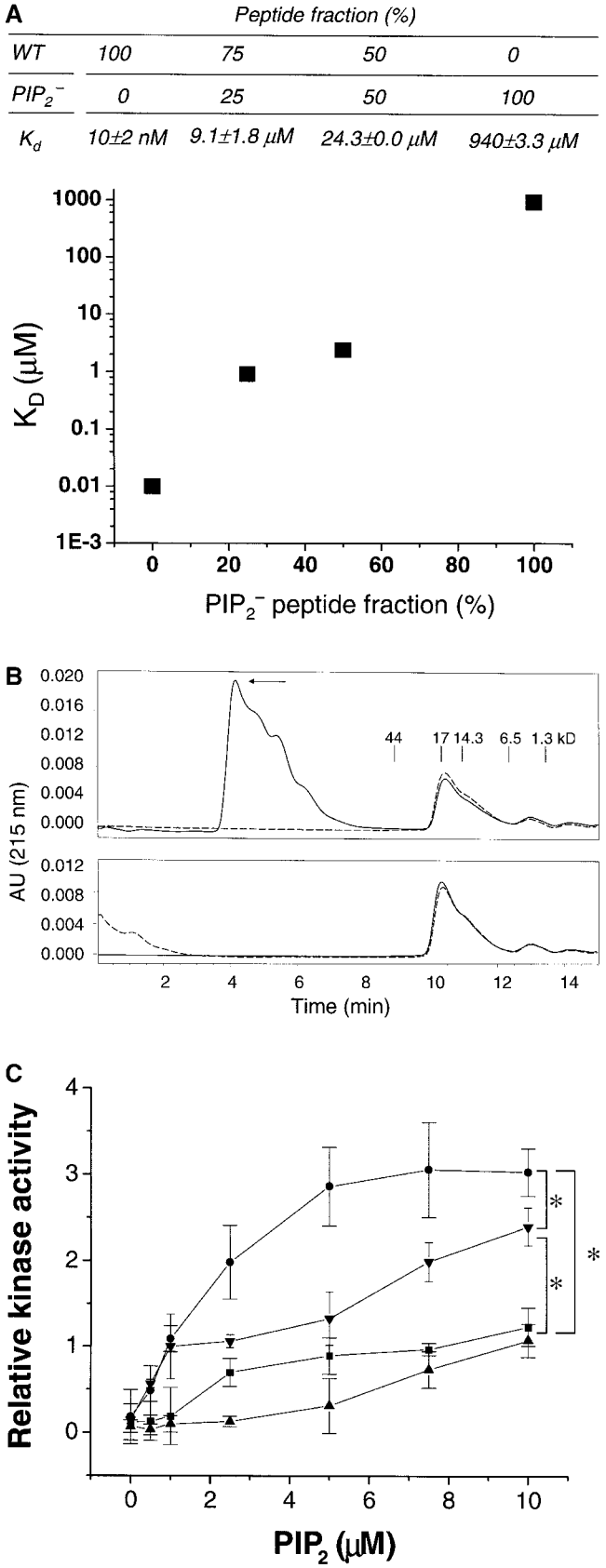

Figure 8. **In vitro experiments with synthetic WT and mutated syndecan-4 cytoplasmic tail peptides.** (A) Dependence of surface plasmon resonance-measured apparent first-order equilibrium constants (K_D) between PIP_2 and PIP_2^-/WT peptide mixtures on PIP_2^- peptide fraction. Note the gradual elevation in K_D value upon increasing the PIP_2^- peptide fraction. (B) Column elution profiles of WT (top) and PIP_2^- (bottom) cytoplasmic tail peptides with (continuous line) and without (dashed line) PIP_2. Note the formation of high-order oligomers by the WT (arrow) but not by the PIP_2^- peptide in the presence of PIP_2. Note also that both peptides are not present as monomers but form smaller oligomers of similar sizes both in the presence and absence of PIP_2. (C) Dependence of the in vitro activity of recombinant PKCα on PIP_2 concentration in the absence (■) and the presence of 1 μM WT (●), PIP_2^- (▲), or PDZ^- (▼) cytoplasmic tail peptides (mean ± SD, $n = 3–6$; $*p < 0.05$). The mean kinase activity measured at 1 μM PIP_2 with 1 μM WT peptide was used as a unitary reference value.

mic tail (Horowitz and Simons, 1998a), we compared the effect of FGF2 stimulation on the phosphorylation level of the PDZ^- mutant to its effect on the S4 variant. FGF2 administration lowered the phosphorylation levels of S4 in a statistically significant manner (Fig. 7) relative to its basal level, in agreement with previously described results (Horowitz and Simons, 1998a), but it did not lower those of the PDZ^- mutant. Moreover, the phosphorylation level of the PDZ^- mutant after FGF2 treatment was significantly higher than its basal level. This increase may reflect the dependence of the phosphorylation level on a dynamic balance between the opposing actions of a kinase and a phosphatase. The dephosphorylation of the PDZ^- mutant would be impaired if the association of syndecan-4 with the putative phosphatase was mediated by a PDZ adaptor protein. Consequently, the activity of the kinase that phosphorylates Ser^{183}, which could conceivably be elevated by FGF2, would be unopposed by the phosphatase, resulting in an effective increase in the phosphorylation level of syndecan-4.

Since it is likely that the PDZ^- mutant and the endogenous syndecan-4 copolymerize, the abolishment of the binding of the putative phosphatase may affect the phosphorylation levels of both syndecan-4 variants. Since the currently available antibodies cannot separate between the endogenous and the exogenous syndecan-4 species, we were able to measure the effect of FGF2 on the phosphorylation level of only the total syndecan-4 population, which was not changed significantly (Fig. 7). This outcome could be attributed to opposing and mutually canceling changes in the phosphorylation levels of the endogenous and PDZ syndecan-4 populations in response to FGF2, thus implying that the expression of the PDZ^- mutant did not significantly affect the phosphorylation level of endogenous syndecan-4.

PIP_2^- mutation reduces syndecan-4 PIP_2-dependent oligomerization and activation of PKCα

The capacity of syndecan-4 to activate PKCα is dependent on its affinity to PIP_2 and on its tendency to oligomerize in the presence of this phosphoinositide (Horowitz and Simons, 1998a). The potent suppression of PKCα activity and of several cell functions by the LQQ mutation implies that the PIP_2^- mutant has a dominant negative effect when expressed on a background of endogenous syndecan-4. Therefore, we investigated the effect of mixing PIP_2^--mutated cytoplasmic syndecan-4 tail peptide with the WT tail peptide on the combined affinity of the mixture to PIP_2 in vitro. As little as 25% of PIP_2^- peptide in the total WT/PIP_2^- mixture increased the apparent K_D of the mixture by three orders of magnitude

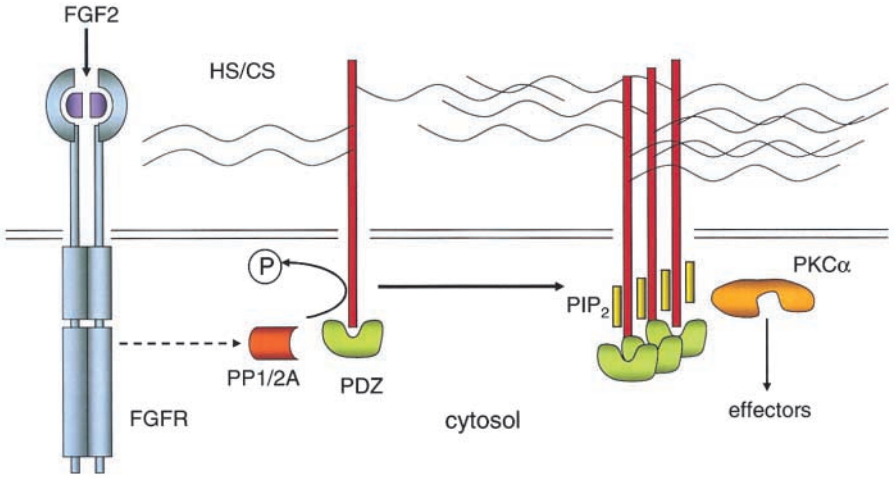

Figure 9. **Schematic representation of FGF2 signal transduction mediated by syndecan-4.** FGFR, FGF2 tyrosine kinase receptor; CS, chondroitin sulfate side chains. See Discussion for details.

compared with that of the WT peptide alone as measured by surface plasmon resonance (Fig. 8 A).

Since syndecan-4–PIP_2 binding is thought to play a role in the oligomerization of syndecan-4 tails (Oh et al., 1997a; Horowitz and Simons, 1998a), we examined the oligomerization capacity of the PIP_2^- peptide. When resolved by column chromatography, the PIP_2^- peptides did not form high-order oligomers in the presence of PIP_2 unlike the WT peptides (Fig. 8 B). However, both peptides formed smaller PIP_2-independent oligomers of a size between tetramers and hexamers. The capacity of the PIP_2 peptide to form low-order oligomers in the same manner as the WT peptide may explain the significantly higher K_D between PIP_2 and the 25%:75% PIP_2^- to WT peptide mixture reported above, since the two peptides could form heterooligomers of a PIP_2 affinity much lower than that of WT homooligomers due to the presence of the PIP_2^- peptide. The decreased affinity of the PIP_2^- peptide to PIP_2 and its lower tendency to oligomerize were accompanied by a large reduction in its capacity to activate PKCα in the presence of PIP_2 relative to the WT peptide (Fig. 8 C). Though the PDZ^- peptide is shorter than the WT peptide only by a single residue, the COOH-terminal alanine, the PKCα activity in its presence at $2.5\ \mu M \leq PIP_2 \leq 10\ \mu M$ was lower in a statistically significant manner than the corresponding activities in the presence of the WT peptide but higher than those of the PIP_2^- mutant.

Discussion

We have described a novel mechanism regulating growth factor signaling, distinctive both for its specificity to FGF2 (versus serum, EGF, and PDGF) and for the pivotal role of syndecan-4. The main feature of this signaling pathway is activation of PKCα by the syndecan-4–PIP_2 complex in response to FGF2 stimulation. This process is controlled by the phosphorylation of S^{183} in the cytoplasmic tail of syndecan-4 that down-regulates the response to FGF2 by preventing PIP_2-dependent oligomerization of syndecan-4 and the subsequent activation of PKCα.

Our working model of this mechanism (Fig. 9) consists of the following steps. (a) FGF2 binding to its high affinity tyrosine kinase receptor induces the activation of a putative serine/threonine protein phosphatase type 1/2A (PP1/2A) (Horowitz and Simons, 1998b), which is associated with the cytoplasmic tail of syndecan-4 through a PDZ adaptor protein. (b) The PP1/2A dephosphorylates Ser^{183} in the membrane proximal domain of the syndecan-4 cytoplasmic tail, which is normally maintained at a high basal phosphorylation level. Since the HS chains carried by proteoglycans can reach estimated lengths of 80 nm (Kato et al., 1994), the dephosphorylation is likely to occur in a trans rather than a cis mode in regard to the syndecan-4 molecule carrying the FGF2-binding HS chain. Since syndecan-4 is a transmembrane protein, this dephosphorylation may similarly occur in the Golgi-residing syndecan-4. (c) Dephosphorylation of syndecan-4 sharply increases its affinity to PIP_2 (Horowitz and Simons, 1998a). In turn, PIP_2 binding facilitates the multimerization of syndecan-4. (d) The clustered syndecan-4–PIP_2 complex activates PKCα, which associates with syndecan-4 through PIP_2 (Horowitz et al., 1999).

The existence of this regulatory mechanism is suggested by our observations that expression of PIP_2^- or PDZ^- syndecan-4 mutants on a background of endogenous syndecan-4 inhibits cell response to FGF2 but not to serum or the HS binding EGF and PDGF AB in a dominant negative manner. In the case of the PIP_2^- mutation, the mistargeting of the mutant syndecan-4 leads to Golgi sequestration of its PDZ-binding partner. The critical role of this sequestration is emphasized by the lack of dominant negative effects of the double PIP_2^-/PDZ^- syndecan-4 mutation. In the case of the PDZ^- deletion, FGF2 treatment would lead to an increase in the extent of syndecan-4 phosphorylation and consequently would decrease PKCα activation due to the low affinity of phosphorylated syndecan-4 for PIP_2 (Horowitz et al., 1999).

A recent study on syndecan-4 knockout mice reported that the proliferative response of skin fibroblasts extracted from these mice did not differ from the response of cells from WT mice (Echtermeyer et al., 2001). The difference between this finding and the significantly reduced proliferation rates of cells expressing the PIP_2^- or PDZ^- syndecan-4 mutants that we observed may stem from each of the following reasons. (a) As explained above, the expression of these mutants interferes with the function of endogenous syndecan-4. This active perturbation of a signaling pathway was not present in the mouse syndecan-$4^{-/-}$ cells. (b) Differences between cell types (fibroblasts versus endothelial cells) used in the two studies. (c) Assuming that Echtermeyer et al. (2001) used the same medium as in their migration assays (the medium used in their proliferation assays is not described), the 2% serum present in this

medium may have contained other growth factors that compensated for the impaired response to FGF2.

PIP_2^- mutation: effect on plasma membrane targeting of syndecan-4

One interesting and unexpected finding in this study is the fact that PIP_2 binding rather than the interaction with a PDZ protein targets syndecan-4 to the plasma membrane. The data supporting this observation include immunofluorescence staining showing reduced expression of the PIP_2^- and PIP_2^-/PDZ^- mutants in the basolateral region and virtual absence of syndecan-4 variants containing the PIP_2^- mutation from the cell surface as demonstrated by FACS. Similarly, deletion of the PDZ motif in the syndecan-2 cytoplasmic tail did not eliminate its incorporation into the plasma membrane (Ethell and Yamaguchi, 1999).

The Golgi apparatus is a known site of PIP_2 synthesis (Godi et al., 1999; Jones et al., 2000), and the involvement of PIP_2 in protein sorting is suggested by preliminary observations (Morrow, M.W. and P. Weidman, 2000. *Mol. Biol. Cell.* 11:S280a). However, the actual targeting mechanism is still unknown. The results of the FACS experiments (Fig. 5 A) show that the PIP_2^- mutation precluded not only the basolateral targeting but also the overall incorporation of syndecan-4 in the plasma membrane.

The dominant negative phenotype exhibited by the PIP_2^- mutant suggests that it disrupts a syndecan-4–dependent protein complex involved in mediating FGF2 signaling. Interestingly, it is the presence of the PIP_2^- mutant and not a mere absence of syndecan-4 from the cell that impairs cellular function. This conclusion is supported by studies of the PIP_2^-/PDZ^- mutant that does not cause a similar dominant negative phenotype, yet it is similarly absent from the plasma membrane (Fig. 4 C), and by a recently described syndecan-4 knockout mouse (Ishiguro et al., 2000). Instead, we propose that the dominant negative effect of the PIP_2^- mutation is caused by sequestration to the Golgi apparatus of a syndecan-4–binding PDZ protein specifically involved in FGF2 (and not serum, EGF, or PDGF) signaling. Assuming that FGF2 signaling requires the presence of this syndecan-4–bound PDZ protein in the basolateral region, the PIP_2^- mutant may compete with endogenous syndecan-4 for binding to the PDZ protein, thus capturing a large part of this protein population at the Golgi apparatus and interfering with its targeting to the plasma membrane and the formation of a syndecan-4–dependent complex.

PDZ binding regulates syndecan-4 phosphorylation in response to FGF2

We have shown that the dominant negative effect of the PDZ^- mutation is associated with increased phosphorylation of the PDZ^- syndecan-4 mutant after FGF2 treatment. The phosphorylation state of syndecan-4 is controlled on one hand by a novel PKC (nPKC) and on the other by a FGF2-activated PP1/2A (Horowitz and Simons, 1998b). Since the phosphorylation level of the PDZ^- mutant was significantly higher than that of S4 after FGF2 treatment, the most likely explanation for this observation is impaired dephosphorylation of the PDZ^- mutant, resulting in unopposed activity of the nPKC. This in turn suggests that the PP1/2A involved in syndecan-4 dephosphorylation forms a complex with syndecan-4 through a PDZ adaptor protein. In the absence of the PDZ-binding motif of syndecan-4, and hence PDZ adaptor binding, the phosphatase would no longer dephosphorylate the PDZ^- mutant. This explanation applies both to the membrane and the Golgi-associated syndecan-4 pools, since the cytoplasmic tail of the latter would protrude into the cytoplasm and be accessible to the phosphatase and kinase.

The hyperphosphorylated PDZ^- mutant has reduced tendencies to oligomerize and bind PIP_2, resulting in a diminished capacity to activate PKCα (Horowitz and Simons, 1998a). Moreover, its presence in the plasma membrane may interfere with the oligomerization, PIP_2 binding, and activation of PKCα by dephosphorylated endogenous syndecan-4. This loss of syndecan-4–dependent activation of PKCα in response to FGF2 may then account for the dominant negative effects of the PDZ^- mutation.

It should be noted that the lower activity of PKCα in the presence of the PDZ^- peptide compared with the WT peptide (Fig. 8 C) leaves open the possibility that the induction of a dominant negative phenotype by the PDZ^- mutation can be caused by reduction in PKCα activity, similar to the PIP_2^- cells. Although it is not obvious how deletion of a single COOH-terminal residue in the cytoplasmic tail of syndecan-4 produces this effect, the deletion could conceivably affect the conformation of the PIP_2-binding motif and hence reduce its affinity to PIP_2.

FGF2 specificity of the syndecan-4 signaling pathway

Another intriguing observation in this study is the apparent FGF2 specificity (versus serum, EGF, and PDGF) of the syndecan-4 signaling pathway. This specificity may stem in part from the choice of functional assays used in this study, since both cell migration (Harrington et al., 1997) and proliferation (Schonwasser et al., 1998; Besson and Yong, 2000) have been linked to the activation of PKCα, the kinase regulated by syndecan-4. However, not all FGF2-induced signaling events may necessarily be regulated in this fashion. The fact that, unlike FGF2, serum stimulation of cell growth and proliferation is not affected by the $PIP_2^-$and PDZ^- syndecan-4 mutants suggests that other growth factors present in serum, such as EGF or PDGF AB, may stimulate cell growth and migration independent of PKCα. The lack of increase in PIP_2-dependent PKCα activation after serum stimulation (Fig. 6 A) agrees with this observation.

Though all syndecans and glypicans can carry HS chains and may, therefore, bind FGF2, only syndecan-4 selectively modulates FGF2 signaling (Volk et al., 1999; Simons and Horowitz, 2001). The unique nature of the syndecan-4–dependent amplification of FGF2 signaling is related to the presence of its cytoplasmic tail, since the expression of chimeras consisting of either glypican-1 (Volk et al., 1999) or syndecan-1 (unpublished data) ectoplasmic domain fused to the transmembrane and cytoplasmic domains of syndecan-4 mimics the positive effects of intact syndecan-4 overexpression on cell proliferation and migration. These findings, together with the results of the current study, suggest that PIP_2 binding and the concomitant ability to activate PKCα underlie the unique capacity of syndecan-4 among the cell surface proteoglycans to regulate FGF2 signaling.

In summary, we describe a novel signal transduction pathway that involves selective regulation of endothelial cell migration and proliferation by FGF2 via syndecan-4.

Materials and methods

cDNA constructs, mutagenesis, and transfection

Syndecan-4 cDNA containing an ectoplasmic HA tag (Shworak et al., 1994) was subcloned into MSCV retroviral vector (Hawley et al., 1994) between its EcoRI and BglII sites. Site-directed mutations were introduced into syndecan-4 cDNA by PCR-mediated oligomutagenesis (QuikChange; Stratagene). The vector was delivered into RFPECs by either retroviral (as described in Volk et al., 1999) or liposome-mediated transfection (LipofectAmine Plus; Invitrogen). In both cases, stably transfected cells were selected by neomycin resistance (0.4 mg/ml Geneticin; Invitrogen). Syndecan-4 expression levels were assessed by immunoblotting cell lysates as described (Horowitz and Simons, 1998a) with 50 mU/ml HRP-conjugated 3F10 HA antibody (Roche).

Alternatively, the HA-tagged syndecan-4 cDNA constructs were inserted between the XhoI and EcoRI restriction sites of a bicistronic mammalian expression plasmid (pIRES2-EGFP; CLONTECH Laboratories) that coexpresses EGFP and the inserted cDNA under a single promoter. RFPECs were stably transfected by LipofectAmine 2000 (Invitrogen) and selected by neomycin resistance as a pooled population. To enrich each pool with cells having high expression levels of the transfected protein, only cells in the top 2–5% of the population as determined by two to three consecutive sorting rounds (see below) were retained and expanded.

Cell function assays

Cells were incubated as described (Horowitz and Simons, 1998a) in M199 medium (Invitrogen) with the indicated supplements. Cell migration was measured by "wounding" assays (Tang et al., 1997) in which cells were grown to subconfluence in 6-well plates and then starved for 24 h in 0.5% serum. The cell layer was scratched with a pipette tip, producing a gap ~2-mm wide. The gap width was measured at marked locations from images taken by inverted microscope (TMS-F; Nikon) immediately after the scratching and again 6 h later at the same locations. Proliferation and tube formation assays were done as described (Volk et al., 1999). All experiments were repeated with two clones of cells stably transfected with each syndecan-4 variant. Neomycin was withdrawn from the culture medium at least 24 h before the cell function assays and before all other experiments with stably transfected RFPECs to prevent artifacts caused by neomycin sequestration of PIP_2 (Gabev et al., 1989).

FACS

To measure the amount of exogenous syndecan-4 present on the cell surface, cells were dissociated from plates (nonenzymatic solution; Sigma-Aldrich), labeled with 1 μg/ml antibody to HA (Roche) followed by 10 μg/ml of anti–rat IgG conjugated to R-PE (Jackson Immunologicals), and sorted automatically (FACScan®; Beckton Dickinson). Detection of the surface expression of both exogenous and endogenous syndecan-4 was done similarly using a 1:50 dilution of antiserum to the ectoplasmic domain of syndecan-4 (Shworak et al., 1994) and 10 μg/ml of anti–rabbit IgG conjugated to Alexa-594 (Molecular Probes). To detect the overall cellular expression of exogenous syndecan-4, cells were scanned at the EGFP-emitted wavelength (488 nm).

Immunofluorescence

RFPECs were plated in chamber slides (Nunc), fixed with 2% formaldehyde in PBS (137 mM NaCl, 4.3 mM $Na_2HPO_4 \cdot 7H_2O$, 2.7 mM KCl, 1.4 mM KH_2PO_4, pH 7.3) for 10 min at room temperature, washed twice with PBS, permeabilized with 0.1% Triton X-100/PBS for 10 min, washed again as above, blocked with 3% BSA (Invitrogen) in PBS for 30 min, and incubated with primary antibodies at the indicated concentrations in 1% BSA in PBS for 3 h. The slides were washed four times as above and incubated for 1 h with 10 μg/ml of the appropriate secondary antibodies conjugated either to Alexa 488 or Alexa 594 (Molecular Probes), washed again as before, and mounted with ProLong medium (Molecular Probes). Slides were imaged by laser-scanning confocal microscopy (Radiance2000; Bio-Rad Laboratories, Inc.).

Immunoprecipitation

Cells were lysed and immunoprecipitated as described (Horowitz and Simons, 1998a,b) using 80 μl anti-HA affinity matrix (Roche) suspension per 750 μl cell lysate. Alternatively, endogenous or HA-tagged syndecan-4 was immunoprecipitated with 10 μl cytoplasmic tail antiserum (Shworak et al., 1994) or with 5 μg HA antibody (3F10; Roche) per 750 μl cell lysate, respectively, and 40 μl suspension of protein G plus/protein A agarose (Oncogene). Where indicated, glycosaminoglycan chains were digested as described (Horowitz and Simons, 1998b).

Surface plasmon resonance

Experiments were performed as described (Horowitz et al., 1999) using 28–amino acid–long (Horowitz and Simons, 1998a) syndecan-4 cytoplasmic tail peptides (Genemed Synthesis) as ligands and PIP_2 (Sigma-Aldrich) as analyte.

Column chromatography

Synthetic syndecan-4 cytoplasmic tail peptides (1 μM) either alone or mixed with PIP_2 (2 μM) in 0.1 M phosphate, pH 7.4, and 20% acetonitrile were injected (22.5 μl) into a 300 × 6 mm silica (5 μm spheres, 60 Å pores) HPLC (Waters, 515 Pump, 2487 Absorbance Detector)-mounted column (YMC). Elution profiles corresponding to light absorbance at 210 nm were recorded digitally (Millennium^{32}; Waters).

Kinase assays

With recombinant PKCα. These were performed either in the presence of PIP_2 or Ca^{2+}, phosphatidylserine, and diolein as described (Horowitz and Simons, 1998a) using recombinant PKCα (120 ng/ml). Kinase activity was quantified by phosphoimaging (Molecular Dynamics) of gel-resolved PKCβI optimal substrate peptide bands. PKC autoinhibitor peptide and Gö6976 were purchased from Calbiochem.

With immunoprecipitated syndecan-4. Syndecan-4 complexes immunoprecipitated as described above with 5 μg HA antibody per 750 μl cell lysate and 40 μl protein G plus/protein A agarose suspension were used for in vitro kinase assays. After washing in 25 mM Tris-HCl (pH 7.4) buffer, the beads were sedimented, and the buffer was removed and replaced with 30 ml kinase assay buffer containing either PIP_2 or Ca^{2+}, phosphatidylserine, and diolein as described (Horowitz and Simons, 1998a). The assay was stopped by adding 10 μl ×4 Laemmli sample buffer (final concentration 2% SDS, 10% glycerol, 0.5% β-mercaptoethanol, 0.004% bromophenol blue, 50 mM Tris-HCl, pH 6.8) and boiling for 4 min. Kinase activity was quantified as in the recombinant PKCα assays.

Measurement of syndecan-4 phosphorylation level

RFPECs in 100-mm plates were grown for 24 h in phosphate-free DME (Invitrogen) supplemented with 0.5% FBS and radiolabeled for 4 h with 0.5 mCi/ml [^{32}P]orthophosphoric acid (New England Nuclear). Cells were washed with tris-buffered saline (137 mM NaCl, 25 mM Tris-HCl, pH 7.4) and scraped off in 0.5 ml lysis buffer (150 mM NaCl, 20 mM NaF, 20 mM $Na_4P_2O_7$, 5 mM EDTA, 5 mM EGTA, 1 mM Na_3VO_4, 1 mM PMSF, 1% Triton X-100, 50 mM Hepes, pH 7.4) supplemented with protease inhibitor cocktail (Complete; Boehringer). Cell lysates were precleared by incubation with 1 μg nonimmune rat IgG (Sigma-Aldrich) and 20 μl protein G plus/protein A agarose bead suspension at 4°C for 1 h. After agarose bead sedimentation, the cleared samples were supplemented with 80 μl of anti-HA affinity matrix bead suspension (Roche) or with 10 μl cytoplasmic tail antiserum (Shworak et al., 1994) and 40 μl suspension of protein G plus/protein A agarose (Oncogene) and incubated in rotating tubes over night at 4°C. The beads were sedimented, washed three times in heparinase digestion buffer (50 mM NaCl, 4 mM $CaCl_2$, 20 mM Tris-HCl, pH 7.4), and glycosaminoglycan chains were digested as described (Horowitz and Simons, 1998b). The immunoprecipitated syndecan-4 core protein was dissociated from the beads by a 10-min incubation in 40 μl Laemmli sample buffer at 95°C. Samples were resolved on 12% tris-glycine gels (Bio-Rad Laboratories), and the bands corresponding to the cytoplasmic tail of syndecan-4 were identified by immunoblotting with a peroxidase-conjugated antibody to the HA tag (Roche). The bands were excised, and the ^{32}P level was measured by scintillation counter (Beckman Coulter).

We thank N. Shworak for syndecan-4 cDNA and antiserum, R. Hawley for MSCV plasmid, John Zeind for help with HPLC, and L. Cantley for recombinant PKCα and useful discussions.

This study was supported in part by the American Heart Association Scientist Development grant 9730282N (to A. Horowitz) and by National Institutes of Health grants HL62289 and P50 HL63609 (to M. Simons).

Submitted: 28 December 2001
Revised: 20 March 2002
Accepted: 26 March 2002

References

Alexander, C.M., F. Reichsman, M.T. Hinkes, J. Lincecum, K.A. Becker, S. Cumberledge, and M. Bernfield. 2000. Syndecan-1 is required for wnt-1-induced mammary tumorigenesis in mice. *Nat. Genet.* 25:329–332.

Baciu, P.C., and P.F. Goetinck. 1995. Protein kinase C regulates the recruitment of syndecan-4 into focal contacts. *Mol. Biol. Cell.* 6:1503–1513.

Bernfield, M., M. Gotte, P.W. Park, O. Reizes, M.L. Fitzgerald, J. Lincecum, and M. Zako. 1999. Functions of cell surface heparan sulfate proteoglycans. *Annu. Rev. Biochem.* 68:729–777.

Besson, A., and V.W. Yong. 2000. Involvement of p21(Waf1/Cip1) in protein kinase C alpha-induced cell cycle progression. *Mol. Cell. Biol.* 20:4580–4590.

Cai, H., U. Smola, V. Wixler, I. Eisenmann-Tappe, M.T. Diaz-Meco, J. Moscat, U. Rapp, and G.M. Cooper. 1997. Role of diacylglycerol-regulated protein kinase C isotypes in growth factor activation of the Raf-1 protein kinase. *Mol. Cell. Biol.* 17:732–741.

Cohen, A.R., D.F. Woods, S.M. Marfatia, Z. Walther, A.H. Chishti, J.M. Anderson, and D.F. Wood. 1998. Human CASK/LIN-2 binds syndecan-2 and protein 4.1 and localizes to the basolateral membrane of epithelial cells. *J. Cell Biol.* 142:129–138.

Echtermeyer, F., M. Streit, S. Wilcox-Adelman, S. Saoncella, F. Denhez, M. Detmar, and P.F. Goetinck. 2001. Delayed wound repair and impaired angiogenesis in mice lacking syndecan-4. *J. Clin. Invest.* 107:R9–R14.

Ethell, I.M., and Y. Yamaguchi. 1999. Cell surface heparan sulfate proteoglycan syndecan-2 induces the maturation of dendritic spines in rat hippocampal neurons. *J. Cell Biol.* 144:575–586.

Ethell, I.M., K. Hagihara, Y. Miura, F. Irie, and Y. Yamaguchi. 2000. Synbindin, A novel syndecan-2–binding protein in neuronal dendritic spines. *J. Cell Biol.* 151:53–68.

Gabev, E., J. Kasianowicz, T. Abbott, and S. McLaughlin. 1989. Binding of neomycin to phosphatidylinositol 4,5-bisphosphate (PIP2). *Biochim. Biophys. Acta.* 979:105–112.

Gallo, R.L., M. Ono, T. Povsic, C. Page, E. Eriksson, M. Klagsbrun, and M. Bernfield. 1994. Syndecans, cell surface heparan sulfate proteoglycans, are induced by a proline-rich antimicrobial peptide from wounds. *Proc. Natl. Acad. Sci. USA.* 91:11035–11039.

Gao, Y., M. Li, W. Chen, and M. Simons. 2000. Synectin, syndecan-4 cytoplasmic domain binding PDZ protein, inhibits cell migration. *J. Cell. Physiol.* 184:373–379.

Godi, A., P. Pertile, R. Meyers, P. Marra, G. Di Tullio, C. Iurisci, A. Luini, D. Corda, and M.A. De Matteis. 1999. ARF mediates recruitment of PtdIns-4-OH kinase-beta and stimulates synthesis of PtdIns(4,5)P2 on the Golgi complex. *Nat. Cell Biol.* 1:280–287.

Grootjans, J.J., P. Zimmermann, G. Reekmans, A. Smets, G. Degeest, J. Durr, and G. David. 1997. Syntenin, a PDZ protein that binds syndecan cytoplasmic domains. *Proc. Natl. Acad. Sci. USA.* 94:13683–13688.

Harrington, E.O., J. Loffler, P.R. Nelson, K.C. Kent, M. Simons, and J.A. Ware. 1997. Enhancement of migration by protein kinase Calpha and inhibition of proliferation and cell cycle progression by protein kinase Cdelta in capillary endothelial cells. *J. Biol. Chem.* 272:7390–7397.

Hawley, R.G., F.H. Lieu, A.Z. Fong, and T.S. Hawley. 1994. Versatile retroviral vectors for potential use in gene therapy. *Gene Ther.* 1:136–138.

Horowitz, A., and M. Simons. 1998a. Phosphorylation of the cytoplasmic tail of syndecan-4 regulates activation of protein kinase Calpha. *J. Biol. Chem.* 273:25548–25551.

Horowitz, A., and M. Simons. 1998b. Regulation of syndecan-4 phosphorylation in vivo. *J. Biol. Chem.* 273:10914–10918.

Horowitz, A., M. Murakami, Y. Gao, and M. Simons. 1999. Phosphatidylinositol-4,5-bisphosphate mediates the interaction of syndecan-4 with protein kinase C. *Biochemistry.* 38:15871–15877.

House, C., and B.E. Kemp. 1987. Protein kinase C contains a pseudosubstrate prototope in its regulatory domain. *Science.* 238:1726–1728.

Hsueh, Y.P., F.C. Yang, V. Kharazia, S. Naisbitt, A.R. Cohen, R.J. Weinberg, and M. Sheng. 1998. Direct interaction of CASK/LIN-2 and syndecan heparan sulfate proteoglycan and their overlapping distribution in neuronal synapses. *J. Cell Biol.* 142:139–151.

Ishiguro, K., K. Kadomatsu, T. Kojima, H. Muramatsu, S. Tsuzuki, E. Nakamura, K. Kusugami, H. Saito, and T. Muramatsu. 2000. Syndecan-4 deficiency impairs focal adhesion formation only under restricted conditions. *J. Biol. Chem.* 275:5249–5252.

Jones, D.H., J.B. Morris, C.P. Morgan, H. Kondo, R.F. Irvine, and S. Cockcroft. 2000. Type I phosphatidylinositol 4-phosphate 5-kinase directly interacts with ADP-ribosylation factor 1 and is responsible for phosphatidylinositol 4,5-bisphosphate synthesis in the golgi compartment. *J. Biol. Chem.* 275: 13962–13966.

Kato, M., H. Wang, M. Bernfield, J.T. Gallagher, and J.E. Turnbull. 1994. Cell surface syndecan-1 on distinct cell types differs in fine structure and ligand binding of its heparan sulfate chains. *J. Biol. Chem.* 269:18881–18890.

Kojima, T., N.W. Shworak, and R.D. Rosenberg. 1992. Molecular cloning and expression of two distinct cDNA-encoding heparan sulfate proteoglycan core proteins from a rat endothelial cell line. *J. Biol. Chem.* 267:4870–4877.

Kolch, W., G. Heidecker, G. Kochs, R. Hummel, H. Vahidi, H. Mischak, G. Finkenzeller, D. Marme, and U.R. Rapp. 1993. Protein kinase C alpha activates RAF-1 by direct phosphorylation. *Nature.* 364:249–252.

Kolch, W., A. Philipp, H. Mischak, E.M. Dutil, T.M. Mullen, J.R. Feramisco, J.L. Meinkoth, and D.W. Rose. 1996. Inhibition of Raf-1 signaling by a monoclonal antibody, which interferes with Raf-1 activation and with Mek substrate binding. *Oncogene.* 13:1305–1314.

Lallena, M.J., M.T. Diaz-Meco, G. Bren, C.V. Paya, and J. Moscat. 1999. Activation of IkappaB kinase beta by protein kinase C isoforms. *Mol. Cell. Biol.* 19: 2180–2188.

Lee, D., E.S. Oh, A. Woods, J.R. Couchman, and W. Lee. 1998. Solution structure of a syndecan-4 cytoplasmic domain and its interaction with phosphatidylinositol 4,5-bisphosphate. *J. Biol. Chem.* 273:13022–13029.

Li, J., L.F. Brown, R.J. Laham, R. Volk, and M. Simons. 1997. Macrophage-dependent regulation of syndecan gene expression. *Circ. Res.* 81:785–796.

Martiny-Baron, G., M.G. Kazanietz, H. Mischak, P.M. Blumberg, G. Kochs, H. Hug, D. Marme, and C. Schachtele. 1993. Selective inhibition of protein kinase C isozymes by the indolocarbazole Go 6976. *J. Biol. Chem.* 268:9194–9197.

Nakamura, N., C. Rabouille, R. Watson, T. Nilsson, N. Hui, P. Slusarewicz, T.E. Kreis, and G. Warren. 1995. Characterization of a cis-Golgi matrix protein, GM130. *J. Cell Biol.* 131:1715–1726.

Nikkari, S.T., H.T. Jarvelainen, T.N. Wight, M. Ferguson, and A.W. Clowes. 1994. Smooth muscle cell expression of extracellular matrix genes after arterial injury. *Am. J. Pathol.* 144:1348–1356.

Oh, E.S., A. Woods, and J.R. Couchman. 1997a. Multimerization of the cytoplasmic domain of syndecan-4 is required for its ability to activate protein kinase C. *J. Biol. Chem.* 272:11805–11811.

Oh, E.S., A. Woods, and J.R. Couchman. 1997b. Syndecan-4 proteoglycan regulates the distribution and activity of protein kinase C. *J. Biol. Chem.* 272: 8133–8136.

Oh, E.S., A. Woods, S.T. Lim, A.W. Theibert, and J.R. Couchman. 1998. Syndecan-4 proteoglycan cytoplasmic domain and phosphatidylinositol 4,5-bisphosphate coordinately regulate protein kinase C activity. *J. Biol. Chem.* 273:10624–10629.

Rapraeger, A.C., A. Krufka, and B.B. Olwin. 1991. Requirement of heparan sulfate for bFGF-mediated fibroblast growth and myoblast differentiation. *Science.* 252:1705–1708.

Schonwasser, D.C., R.M. Marais, C.J. Marshall, and P.J. Parker. 1998. Activation of the mitogen-activated protein kinase/extracellular signal-regulated kinase pathway by conventional, novel, and atypical protein kinase C isotypes. *Mol. Cell. Biol.* 18:790–798.

Shworak, N.W., M. Shirakawa, R.C. Mulligan, and R.D. Rosenberg. 1994. Characterization of ryudocan glycosaminoglycan acceptor sites. *J. Biol. Chem.* 269:21204–21214.

Simons, M., and A. Horowitz. 2001. Syndecan-4-mediated signalling. *Cell. Signal.* 13:855–862.

Songyang, Z., A.S. Fanning, C. Fu, J. Xu, S.M. Marfatia, A.H. Chishti, A. Crompton, A.C. Chan, J.M. Anderson, and L.C. Cantley. 1997. Recognition of unique carboxyl-terminal motifs by distinct PDZ domains. *Science.* 275:73–77.

Tang, S., K.G. Morgan, C. Parker, and J.A. Ware. 1997. Requirement for protein kinase C theta for cell cycle progression and formation of actin stress fibers and filopodia in vascular endothelial cells. *J. Biol. Chem.* 272:28704–28711.

Volk, R., J.J. Schwartz, J. Li, R.D. Rosenberg, and M. Simons. 1999. The role of syndecan cytoplasmic domain in basic fibroblast growth factor-dependent signal transduction. *J. Biol. Chem.* 274:24417–24424.

Wang, A., M. Nomura, S. Patan, and J.A. Ware. 2002. Inhibition of protein kinase Calpha prevents endothelial cell migration and vascular tube formation in vitro and myocardial neovascularization in vivo. *Circ. Res.* 90:609–616.

Woods, A., and J.R. Couchman. 1994. Syndecan 4 heparan sulfate proteoglycan is a selectively enriched and widespread focal adhesion component. *Mol. Biol. Cell.* 5:183–192.